Reactivity of Transition-Metal Cluster Carbides Which Have an Exposed Carbon Atom

Sunil D. Wijeyesekera, Roald Hoffmann,* and Charles N. Wilker

Department of Chemistry and Materials Science Center, Cornell University, Ithaca, New York 14853

Received August 31, 1983

In this paper we study the reactivity of butterfly and square-pyramidal transition-metal cluster carbides, compounds which are interesting because they have a sterically exposed carbon atom. First we discuss the stability of these compounds which have such an unusual coordination for carbon. Next we use perturbation theory arguments to discuss the relative reactivities of different sites on the butterfly cluster and of the carbon site on the square-pyramidal cluster. The results parallel the experimentally obtained products; in particular the carbon atom is not electronically the most favored site of attack. The orbital explanation of these trends gives us further insight into bonding in the cluster. We also discuss electron counting and π-bonding in the product of attack on the cluster and consider some relevant data on transition-metal and transition-metal-carbide surfaces.

I. Introduction

There exists a remarkable class of compounds, cluster carbides in which a carbon atom is completely exposed on one side of the molecule. The first known example was $Fe_5(CO)_{15}C$ discovered by Braye and Dahl in 1962.[1] The iron framework is square pyramidal **1**, so that carbon is

$[Fe(CO)_3]_5C$

1

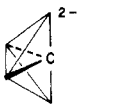

$[Fe(CO)_3]_4C^{2-}$

2

bonded to nothing below the square base. Over the years a number of isostructural carbides were found, and their chemistry was determined.[2] In 1980 a new cluster, $Fe_4(CO)_{12}C^{2-}$, was isolated in which four iron atoms form a butterfly framework.[3] Again the carbon atom which lies halfway in between the wing tips, **2**, is asymmetrically bonded. In these structures, as drawn by us, each unlabeled vertex is an iron atom carrying three carbonyls, $Fe(CO)_3$.

At first sight, it seems strange that these carbides should exist at all. Certainly, nothing in the realm of organic chemistry would indicate such an asymmetric environment for carbon. On the other hand, our experience with bulk carbides[4] has been that it is not a good idea to make comparisons between the valence of carbon in carbides and the valence of carbon in organic compounds. Perhaps a better comparison is to surface chemistry. Much effort in recent years has been devoted to preparing clean metal surfaces. This is of course a very important endeavor if one is to understand details of how a metal surface catalyzes reactivity on an atomic scale; however, it shows that a clean metal surface is not a very stable entity. One of the most pervasive impurities found on surfaces is carbon. Anyone who has ever tried to clean an iron surface[5] can convince him/herself that carbon binds very strongly to metal surfaces and stabilizes them, just as carbon stabilizes these surfacelike clusters.

We might also expect the carbon atom to be a site of attack by other ligands. In fact, a good deal is known about the chemistry of both of these classes of compounds. Two classes of reaction undergone by five-metal-atom clusters are (a) ligand substitution; for example, PR_3 substitutes CO,[2c] and (b) addition of a ligand to the metal framework, for example, I^- adds to $Ru_5(CO)_{15}C$. In this case there is a formal addition of electrons to the metal skeleton, causing it to change to the new geometry **3**. There is, as yet, no example in which an attacking ligand attaches itself to carbon.

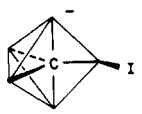

3

In contrast, there are three known examples of addition to the carbide carbon atom in $Fe_4(CO)_{12}C^{2-}$ or a closely related molecule. Attack by an acid gives first a monohydride in which I is attached to the metal framework and then a dihydride in which the second H is attached to carbon (**4**).[7] The dihydride has an extremely long C–H

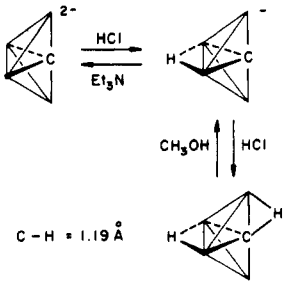

4

(1) Braye, E. H.; Dahl, L. F.; Hubel, W.; Wampler, D. L. *J. Am. Chem. Soc.* **1962**, *84*, 4633–4639.

(2) For two recent reviews see: (a) Muetterties, E. L. *Prog. Inorg. Chem.* **1981**, *28*, 203–238. (b) Johnson, B. F. G.; Lewis, J.; Nelson, W. J. H.; Nicholls, J. N.; Vargas, M. D. *J. Organomet. Chem.* **1983**, *249*, 252–272. Other references are: (c) Gourdon, A.; Jeannin, Y. *C. R. Seances Acad. Sci. Ser. 2* **1982**, *295*, 1101–1104. (d) Farrar, D. H.; Jackson, P. F.; Johnson, B. F. G.; Lewis, J.; Nicholls, J. N.; McPartlin, M. *J. Chem. Soc., Chem. Commun.* **1981**, 415–416. (e) Johnson, B. F. G.; Lewis, J.; Nicholls, J. N.; Puga, J.; Whitmire, K. H. *J. Chem. Soc., Dalton Trans.* **1983**, 787–797.

(3) (a) Boehme, R. F.; Coppens, P. *Acta Crystallogr. Sect. B* **1981**, *37*, 1914–1916. (b) Davis, J. H.; Beno, M. A.; Williams, J. M.; Zimmie, J. A.; Tachikawa, M.; Muetterties, E. L. *Proc. Natl. Acad. Sci. U.S.A.* **1981**, *78*, 668–671.

(4) Wijeyesekera, S. D.; Hoffmann, R., *Organometallics*, preceding paper in this issue.

(5) Ertl, G.; Grunze, M.; Weiss, M. *J. Vac. Sci. Technol.* **1976**, *13*, 314–317.

(6) Jackson, P. F.; Johnson, B. F. G.; Lewis, J.; Nicholls, J. N.; McPartlin, M.; Nelson, W. J. H. *J. Chem. Soc., Chem. Commun.* **1980**, 564–566.

(7) (a) Tachikawa, M.; Muetterties, E. L. *J. Am. Chem. Soc.* **1980**, *102*, 4541–4542. (b) Beno, M. A.; Williams, J. M.; Tachikawa, M.; Muetterties, E. L. *Ibid.* **1981**, *103*, 1485–1492; **1980**, *102*, 4542–4544. (c) Holt, E. M.; Whitmire, K. H.; Shriver, D. F. *J. Organomet. Chem.* **1981**, 213, 125–137.

0276-7333/84/2303-0962$01.50/0

bond and is often mentioned in discussions of C–H activation.[8] Attack by CH_3^+[9] presents a different twist. The product of attack has CH_3^+ attached to the carbide carbon atom but with the metal framework tetrahedral. What a difference the apparently minor perturbation (CH_3^+ replacing H^+) makes! The second example is due to Bradley, who is responsible for a marvelous reaction in which $Fe_6(CO)_{16}C^{2-}$ is used to make an ester from CO and CH_3OH.[10] Part of his reaction scheme[11] is shown in **5** (all

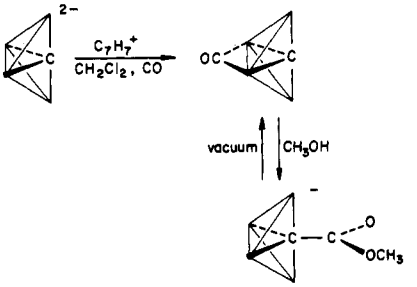

5

intermediates shown have been isolated). Carbon monoxide adds to the metal framework in the presence of $C_7H_7^+$, an oxidizing agent. In this case, addition of CO is accompanied by a loss of charge such that there is no formal addition of electrons to the cluster and no change in the geometry of the metal framework. Addition of methanol to $Fe_4(CO)_{13}C$ gives a product in which the carbide carbon atom is attached to a carbomethoxy ligand.

Hence, the carbon atom in a four-metal-atom cluster is more reactive than the carbon atom in a five-metal-atom cluster, but even in this case the initial product has the ligand attached to the metal framework. A relevant question is whether this structural preference is determined by the relative reactivities of the different sites on the cluster. It is perfectly plausible that ligand attack on carbide carbon is followed by migration around the cluster, provided that this migration is facile. Hydrogen migration is known to be facile, even on an NMR time scale.[7b] There are also examples of migration of CO from carbon to a metal framework,[12] as well as many examples of facile CO migration around metal clusters. In this case the structural preference would reflect only thermodynamic considerations of the various products. The reactivity of the carbide cluster is the subject of our theoretical study.

II. Details of the Calculations

All calculations were performed by using the extended Hückel[13] method, with parameters from previous work.[14]

A C_{3v} $Fe(CO)_3$ cluster was chosen with the angle OC–Fe–CO = 90° (experimental values are in the range 90–100°).[3a] Four $Fe(CO)_3$ clusters were arranged in a butterfly around carbon with the experimental values used for $(Fe–C)_z$ = 1.80 Å, $(Fe–C)_{xy}$ = 1.96 Å, and $(Fe–Fe)_{xy}$ = 2.53 Å (see **6**). The other Fe–Fe bonding distances are forced

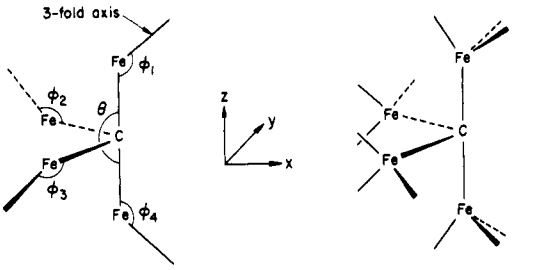

6 **7**

to be 2.62 Å.[15] Concerning the four $Fe(CO)_3$ fragments, we now (a) varied the angles ϕ_i subtended by the threefold axes of the fragments and (b) rotated the fragment around its threefold axis. ϕ_1 and ϕ_4 were varied within the xz plane; ϕ_2 and ϕ_3 were varied within the xy plane. Certain ϕ angles optimize metal-to-carbon bonding; others optimize metal-to-metal bonding. The angles we chose were a compromise: $\phi_1 = \phi_4 = 155.38°$, $\phi_2 = \phi_3 = 165°$. These values are close to the experimental angles[3a] for $Fe_4(CO)_{12}C^{2-}$: $\phi_1 = 154.5°$, $\phi_2 = 166.4°$, and $\phi_3 = 164.2°$. Of course, steric reasons can cause the optimal values of ϕ to be very different when additional ligands are bonded to the cluster. Finally, the fragments were rotated around their threefold axes until a minimum was obtained in the total energy corresponding to the C_{2v} geometry (**7**).

For $Fe_5(CO)_{15}C$, we used the same values for the metal-to-carbon distance; i.e., $(Fe–C)_z$ = 1.96 Å, $(Fe–C)_{xy}$ = 1.80 Å. All angles Fe–C–Fe were ideal. The threefold axes of the four fragments in the xy plane were bent down ($\phi_2 = \phi_4 = 170°$, and $\phi_3 = \phi_5 = 162°$) (**8**). Rotation of carbonyls

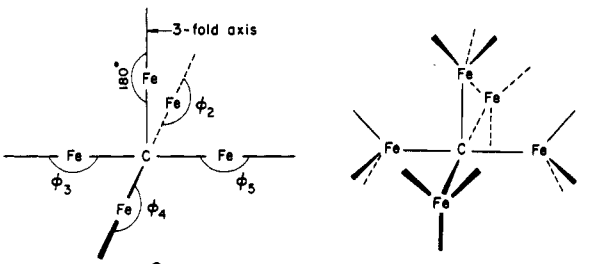

8 **9**

around the threefold axis was constrained to maintain an xz mirror plane, and a minimum energy geometry obtained was **9**.

In both cases the position of the carbide carbon atom was idealized. For $Fe_4(CO)_{12}C^{2-}$, carbon was chosen to bisect the edge of the wing ($\theta = 180°$). Actually $\theta = 176.3°$, and the carbon atom moves slightly out of the wings of the butterfly. For $Fe_5(CO)_{15}C$, carbon was chosen to lie in the plane of the four basal Fe atoms, whereas it is actually displaced slightly (0.1–0.2 Å) below the plane.

III. $Fe_4(CO)_{12}C^{2-}$

Before considering the reactivity of the butterfly cluster, it helps to have some knowledge of its molecular orbitals. The bonding to carbon is highlighted by showing an interaction diagram, Figure 1, for the formation of $Fe_4(CO)_{12}C$ from $Fe_4(CO)_{12}$ and carbon.

$Fe_4(CO)_{12}$ can be considered to be made up of four $Fe(CO)_3$ fragments. The molecular orbitals of the fragment

(8) For a theoretical discussion of C–H activation in this case, see: (a) Housecroft, C. E.; Fehlner, T. P. *Organometallics* **1983**, *2*, (b) Gavin, R. M.; Reutt, J.; Muetterties, E. L. *Proc. Natl. Acad. Sci. U.S.A.* **1981**, *78*, 3981–3985.

(9) Holt, E. M.; Whitmire, K. H.; Shriver, D. F. *J. Am. Chem. Soc.* **1982**, *104*, 5621–5626.

(10) (a) Bradley, J. S.; Ansell, G. B.; Hill, E. W. *J. Am. Chem. Soc.* **1979**, *101*, 7147–7149. (b) Rawls, R. *Chem. Eng. News* **1980**, *58*, Apr 28, 27–28.

(11) (a) Bradley, J. S.; Ansell, G. B.; Leonowicz, M. E.; Hill, E. W. *J. Am. Chem. Soc.* **1981**, *103*, 4968–4970. (b) Bradley, J. S.; Hill, E. W.; Ansell, G. B.; Modrick, M. A. *Organometallics* **1982**, *1*, 1634–1639.

(12) Kolis, J. W.; Holt, E. M.; Drezdon, M.; Whitmire, K. H.; Shriver, D. F. *J. Am. Chem. Soc.* **1982**, *104*, 6134–6135.

(13) (a) Hoffmann, R. *J. Chem. Phys.* **1963**, *39*, 1397–1412. (b) Hoffmann, R.; Lipscomb, W. N. *Ibid.* **1962**, *36*, 2179–2189, 2189–2195.

(14) Summerville, R. H.; Hoffmann, R. *J. Am. Chem. Soc.* **1978**, *98*, 7240–7254.

(15) We initially did the calculations with all Fe–Fe distances the same and all Fe–C distances the same. The differences in overlap population correctly predicted which bonds should shorten.

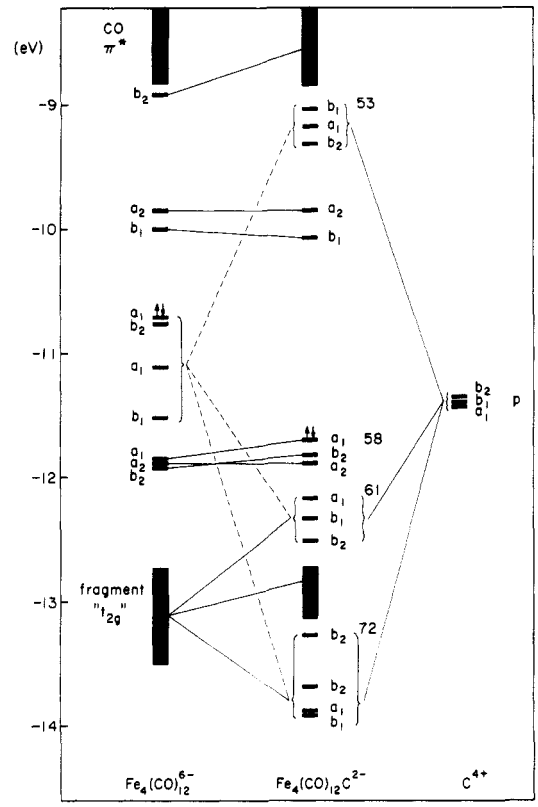

Figure 1. Interaction diagram for the formation of C_{2v} $Fe_4(CO)_{12}C$ from $Fe_4(CO)_{12}$ and carbon. Carbon s orbitals are off-scale. The orbitals of the carbide are numbered from the top down.

are well-known:[16] they consist of a frontier set—the linear combinations of three orbitals directed toward the missing sites of an octahedron—above the remnants of the octahedral t_{2g} set (three orbitals). The t_{2g} set spreads into a narrow band due to metal-to-metal bonding, the frontier set into a wide band. The HOMO–LUMO gap occurs inside the frontier set: a cluster with charge 6– contains seven occupied orbitals in agreement with the calculations of Lauher,[17] as well as with those for the isolobal nido boron hydride.[18]

Bonding with carbon has been discussed in great detail for octahedral and trigonal-prismatic carbides.[4] Interaction of carbon s and p orbitals in Figure 1 occurs primarily with four occupied frontier orbitals of symmetry a_1, a_1, b_1, and b_2 (the molecule has symmetry C_{2v}). The orbitals of the carbide have been numbered from the top down. Carbon s lies very low in energy and is not shown. The other three bonding orbitals (73–75) lie below the t_{2g} set. The three HOMO's (58–60) are the metal-to-carbon nonbonding remnants of the occupied frontier set. Below them lies the t_{2g} set (61–72), except that the top three and the bottommost members of this set contain a substantial carbon content and are shown separately. The reason these orbitals have a high carbon content is that substantial overlap does exist between the t_{2g} set and carbon, especially when threefold axes of the $Fe(CO)_3$ fragments do not point toward carbon. Among the unoccupied orbitals, the LUMO's (56–57) are metal-to-carbon nonbonding, but there is a set of metal-to-carbon antibonding orbitals (53–55) above them. Actually, most metal-to-carbon antibonding is in orbitals that are off-scale.

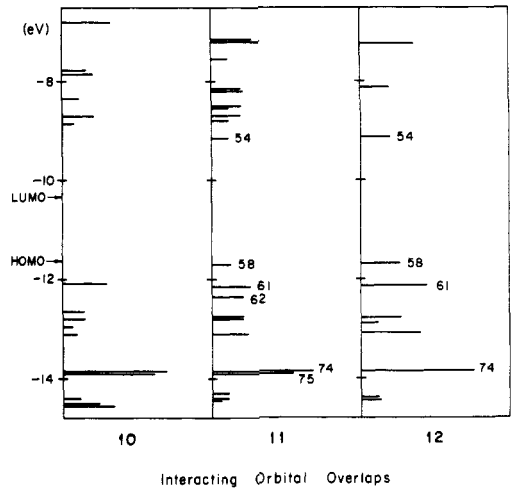

Figure 2. Interacting orbital overlaps of the carbide orbitals with a model hydrogenic wave function for the structures **10–12**. The HOMO and LUMO shown are for $Fe_5(CO)_{15}C$. Numbering for the butterfly cluster corresponds to Figure 1.

The most impressive feature of the carbide is a HOMO–LUMO gap of 1.7 eV. This is remarkably high for a molecule this size in which no approximations (such as substituting H for CO) have been made. Note also how carbon stabilizes the molecule by opening up the HOMO–LUMO gap.

IV. Reactivity with a Model Nucleophile or Electrophile

In this section we use a model hydrogenic orbital i, whose energy E_i is variable, as a probe of reactivity in butterfly and square-pyramidal clusters. Second-order perturbation theory[19] and the extended Hückel approximation tell us that orbital i will interact with each of the orbitals j of the cluster, in a pairwise additive manner, according to the formula $S_{ij}^2/(E_i - E_j)$.

There are many reasons for separating the overlap term S_{ij} from the energy term $E_i - E_j$. One reason is to make it easier to understand what would happen to a range of nucleophiles with different E_i. Another is to take account of the fact that our knowledge of these E_i's is very imperfect; if the result we get is dependent on small changes in the energy of the nucleophile, we should be cautious. The problem with separating out the overlap term is one of presentation: there may be a large number of orbitals of a molecule that interact with a nucleophile. This is true of large molecules such as the one we are considering; it is specially true of solids. Hence, we adopt a solution from solid-state physics, the same one we adopted when discussing bulk carbides. We draw the orbital energies in the way we normally construct an MO diagram, except that the line drawn for each orbital is weighted by the overlap of that orbital with the probe. For the bulk carbides,[4] orbitals were weighted either by their percent carbon to give a projection of carbon or by their overlap population to give a COOP curve. In our case we have constructed an interacting orbital overlap (IOO) curve; six of these curves are plotted in Figures 2 and 3.

The geometries of attack corresponding to each profile are discussed in **10–15**. Carbon-to-nucleophile distances in **10**, **11**, **12**, and **15** are 2.0 Å. Carbon-to-nucleophile and

(16) Albright, T. A.; Hofmann, P.; Hoffmann, R. *J. Am. Chem. Soc.* **1977**, *99*, 7546–7557.
(17) Lauher, J. W. *J. Am. Chem. Soc.* **1978**, *100*, 5305–5315.
(18) (a) Wade, K. *Chem. Commun.* **1971**, 792–793. (b) Wade, K. *Inorg. Nucl. Chem. Lett.* **1972**, *8*, 559–562. (c) Wade, K. "Electron Deficient Compounds"; Nelson: London, 1971. (d) Mingos, D. M. P. *Nature Phys. Sci.* **1972**, *236*, 99–102.
(19) For a more explicit discussion of second-order perturbation theory applied to the interaction between two orbitals, see: Jorgensen, W. L.; Salem, L. "The Organic Chemist's Book of Orbitals"; Academic Press: New York, 1977; pp 10–11.

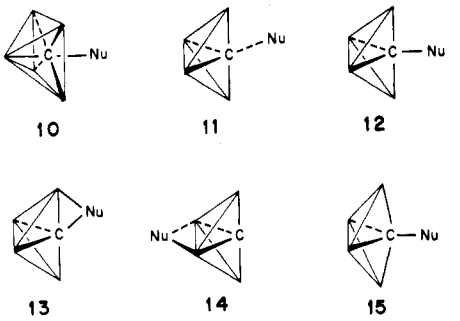

iron-to-nucleophile distances in **13** are 2.4 Å. In this case the threefold axis of the bridged $Fe(CO)_3$ unit is bent back (ϕ_1 = 165.38°). The iron-to-nucleophile distance in **14** is 2.7 Å.

We start our discussion of these curves with some general comments about the reactivity of the butterfly cluster. As already mentioned, this cluster has a very large HOMO–LUMO gap of 1.7 eV, which tends to make it stable to attack. Figures 2 and 3 indicate that, in addition, most of its overlap with an incoming probe orbital is through occupied orbitals. This is in accord with the experimental facts described earlier: attack on the cluster is either with an electrophile (H^+) or with a nucleophile and an oxidizing agent (CO and $C_7H_7^+$).

The reason a nucleophile cannot act alone is that its major interaction is with occupied orbitals and is repulsive. Part of this repulsive energy is contained in a rising HOMO. When the energy of the HOMO rises above the energy of the LUMO on an oxidizing agent, electrons are transferred to the oxidizing agent, and there is a favorable bonding interaction between the HOMO and the nucleophile. If this orbital of the oxidizing agent lies inside the HOMO–LUMO gap of the carbide, the barrier to attack of a nucleophile is reduced, as shown schematically in **16**.

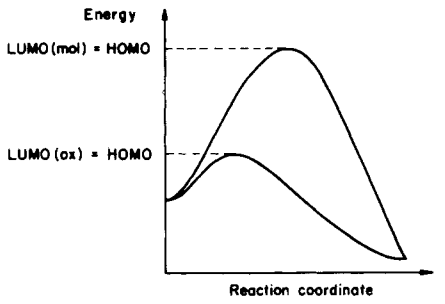

16

The essence of this and the following arguments does not change if electron transfer to the oxidizing agent occurs before attack of CO on the butterfly carbide.

For a given nucleophile, which feature of a molecule makes this electron transfer efficient? To answer this question, we have constructed interaction diagrams in Figure 4 for the attack of H^- (H_{ii} = −13.6 eV) either on the carbon atom, **12**, or on the back iron-to-iron bond, **14**. The major difference between the two interaction diagrams is that a much higher percentage of the repulsive energy of interaction is directed into the HOMO during attack on the iron-to-iron bond. IOO curves also show this difference. For attack on the back iron-to-iron bond the major interaction is with the HOMO (58). For attack on carbon the major interaction is with a deeper orbital (74) which is one of the iron-to-carbon bonds.

Hence, to understand the oxidizing-agent-assisted attack of a nucleophile, we need to consider the distribution of probe overlaps among *occupied* states of the carbide. A large overlap of the probe with states near the Fermi level

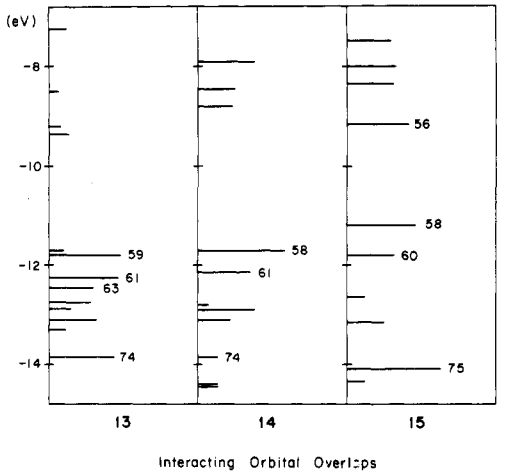

Figure 3. Interacting orbital overlaps of the carbide orbitals with a model hydrogenic wave function for the structures **13–15**. Numbering for the butterfly cluster corresponds to Figure 1.

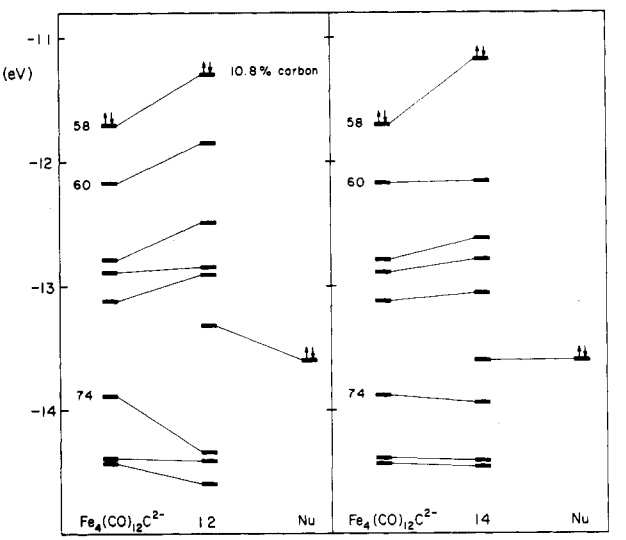

Figure 4. Interaction of a model nucleophile (H_{ii} = −13.6 eV) with the butterfly carbide: left, attack on carbon, **12**; right, attack on the back Fe–Fe bond, **14**. Only orbitals of a_1 symmetry are shown.

is favorable. We now extend this concept to ask how we might favor attack on the carbon atom of $Fe_4(CO)_{12}C^{2-}$. If we compare the two asymmetric attacks **11** and **13** with direct attack **12**, we see that the best attack is **13**, across an iron-to-carbon axial bond. The reason for this is a good overlap with an orbital (59) which is near the HOMO.

We also have a means of comparing direct attack on the carbon atom of a butterfly cluster with a similar attack on a square-pyramidal cluster. The HOMO–LUMO gap is actually 1.3 eV in the square-pyramidal cluster, smaller than it is in the butterfly cluster. However, in the square-pyramidal cluster the HOMO does not have the correct, a_1 symmetry to interact with a nucleophile, and hence the effective HOMO is an orbital $^1/_2$ eV below the real HOMO. More importantly, a larger percentage of the overlap of the square pyramid with a probe is with low-lying iron–carbon bonding orbitals. The net result is that attack on the carbide carbon atom of the square-pyramidal cluster is less favorable.

It is helpful to have a numerical criterion to summarize these results. Unfortunately, we are not able to draw a complete reaction profile since (i) the energy of the oxidizing agent is uncertain, and (ii) we are comparing apples with oranges: Fe–H bonds with C–H bonds. A criterion that gets around these objections, one that we shall use,

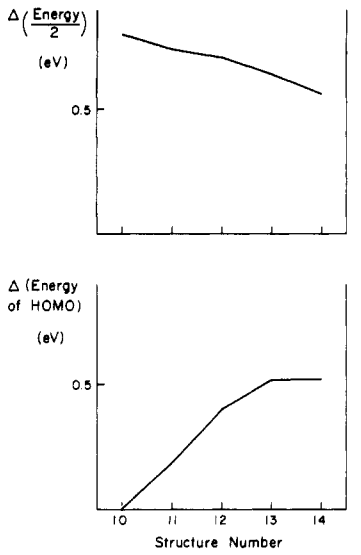

Figure 5. Change in total energy, and change in the energy of the HOMO on interacting $Fe_4(CO)_{12}C^{2-}$ with H^- (H_{ii} = −13.6 eV).

is the percentage of repulsive energy that is channeled into the HOMO. The higher the percentage of repulsive energy in the HOMO the faster it transfers its electrons to the oxidizing agent and the lower the barrier to attack.

The components of this ratio are illustrated separately in Figure 5. As we go from left to right in this figure, **10**–**14**, the repulsive change in the total energy of the system decreases, but the energy of the HOMO rises. Hence, the structures exhibit increasing reactivity from left to right in this figure. The reader will notice that this ordering is in accord with the qualitative picture implied by the interacting orbital overlap curves.

We can also change the energy of the probe to model a more electronegative ligand. The probe energy of −13.6 eV used in Figure 5 is close to the energy of the donor orbital on a CO or PH_3 ligand. In contrast, we use −11.5 eV in Figure 6; this energy is typical of the lone pair of I^- or CH_3^-. This new probe is close in energy to the HOMO of the carbide and hence has a greater "reactivity" with the carbide; i.e., the change in total energy is approximately the same as in Figure 5, but the rise of the HOMO is greater. Hence, if we take two electrons out of this system, we obtain a large attractive energy. Secondly, the trend with different structures is the same as in Figure 5, but the differences are less marked. In other words, the "selectivity" of the probe is much less.

It is interesting to compare our results to previous theoretical discussions of these two carbides. Shriver et al.[20] studied model carbides in which three CO ligands were replaced by one H. They correlated the greater reactivity of the carbon atom of a butterfly cluster when compared to that of the carbon atom of a square-pyramidal cluster to the fact that the HOMO of the butterfly carbide contains a significant charge on the carbon atom. We agree with this result; however, we do not agree with them that the HOMO–LUMO gap is less in the butterfly cluster. Housecroft and Fehlner[8] did Fenske–Hall calculations on the *product* of interaction of a hydrogen atom with the butterfly cluster and showed that there is a greater overlap of hydrogen with the set of frontier orbitals of the cluster when hydrogen bridges an Fe–C bond as in **13** than when it is attached symmetrically to carbon. Our calculations on a reactant-like geometry are in agreement.

(20) Kolis, J. W.; Basolo, F.; Shriver, D. F. *J. Am. Chem. Soc.* **1982**, *104*, 5626–5630.

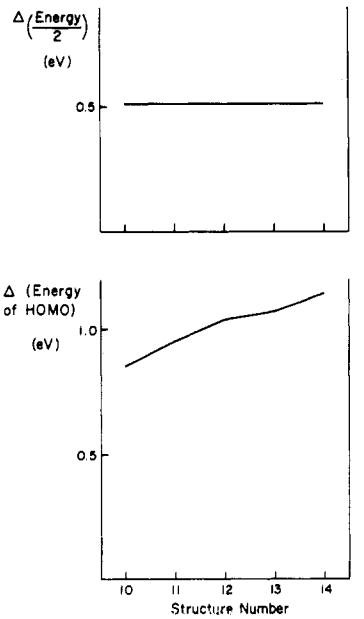

Figure 6. Change in total energy, and change in the energy of the HOMO on interacting $Fe_4(CO)_{12}C^{2-}$ with H^- (H_{ii} = −11.5 eV).

This trend in reactivity for different structures is also in excellent agreement with the experimentally determined thermodynamic products. In our introduction, we stated that (i) initial attack occurs on the back iron-to-iron bond as in **14**; (ii) in the case of H^+ attack, the product of attack on carbon was asymmetric as in **13**. There are also other examples of a product in which a ligand is bonded to the carbide in a manner analogous to **13**. These are the attachment of OCH_3^- to $HFe_4(CO)_{12}C^+$[7c] and the attachment of the carbene $C(H)(t\text{-}Bu)^{2-}$ to $HNiOs_3Cp(CO)_9C^{2+}$.[21] A counterexample exists from the work of Bradley (**5**), the attachment of $CO(OCH_3)^-$ to $Fe_4(CO)_{12}C$, which is in accord with **12** (this data is summarized in Table I). The reason for this exception may be steric. In any case it is not necessary to invoke mobility around the cluster to explain the preferred products as was implied in our discussion at the end of the Introduction.

V. Orbital Explanation

We now derive an orbital explanation of the above trends. The most surprising result of the previous section was the low reactivity of the carbide carbon atom. In order to explain this result, it is predagogically useful to compare the carbide to its organic analogue, butterfly CH_4. Butterfly CH_4 does not exist, and a Walsh diagram for the transformation tetrahedral to butterfly depicted in **17**

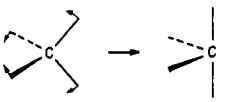

17

quickly explains why this is so. Of the three p orbitals on carbon, p_z becomes more bonding on going from tetrahedral to butterfly, but p_y rises in energy. These two orbitals cancel one another out leaving the largest effect, that due to the p_x orbital which very rapidly loses bonding on one side of the molecule and becomes directed towards the

(21) (a) Sappa, E.; Tiripicchio, A.; Camellini, M. T. *Inorg. Chim. Acta* **1980**, *41*, 11–17. (b) Sappa, E.; Tiripicchio, A.; Camellini, M. T.; Carty, A. J., to be submitted for publication.

(22) (a) Wong, K. S.; Scheidt, W. R.; Fehlner, T. P. *J. Am. Chem. Soc.* **1982**, *104*, 1111–1113. (b) Fehlner, T. P.; Housecroft, C. E.; Scheidt, W. R.; Wong, K. S. *Organometallics* **1983**, *2*, 825–833.

Table I. Structural Parameters of $Fe_4(CO)_{12}C^{2-}$, $HFe_4(CO)_{12}C^-$, and Their Derivative Compounds in Which an Extra Ligand Is Attached to Carbon or to the Metal Framework

framework	ligand	θ, deg	$(Fe-C)_z$, Å	$(Fe-C)_{xy}$, Å	structure	ref
$Fe_4(CO)_{12}C$	$2e^-$	176.3	1.80	1.97		3
	CO	176.0	1.80	1.99	14	11a
	$CO(OCH_3)^-$	147.9	2.02	1.95	12	10a
	$FeBr_2^{2-}$				11	11b
$HFe_4(CO)_{12}C^+$	$2e^-$	174.0	1.80	1.99		7a
	H^- [b]	170.5	1.82, 1.92[a]	1.95	13	7a
	OCH_3^-	162.4	1.83, 2.14[a]	1.96	13	7c
$HNiRu_3Cp(CO)_9C^{2+}$	$CH(t\text{-}Bu)^{2-}$	153.9			13	21

[a] The bridged axial bond is longer. [b] The isoelectronic BH_2 complex exists in which the geometry of the B-H bond is similar to that of the C-H bond in **13**.[22]

empty coordination site, **18**. It is the p_x orbital which is responsible for CH_4 not having a butterfly structure.

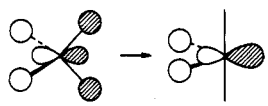

18

If such a "lone pair" existed in the butterfly carbide, we would expect our probe to feel a large interaction with an orbital near the HOMO. In fact, probe **12** finds the major p_x character to be in the much lower energy region of the iron–carbon bonds. The reason is that the carbon "lone pair" is lowered in energy through π *bonding* with iron orbitals (**19**). This π interaction is not possible when carbon is attached only to hydrogen with its s orbital.

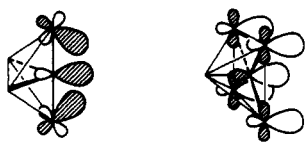

19 **20**

We can obtain both theoretical and experimental measures of the strength of this π bond. The theoretical measure is that the overlap population (bonding) of carbon p_x with the rest of the cluster is not less than the overlap population of carbon p_y with the rest of the cluster. Actual contributions of the different carbon orbitals to the total overlap population are s = 0.6282, p_x = 0.4944, p_y = 0.5014, and p_z = 0.6324.

The experimental measure is structural; it is summarized in Table I. In those compounds in which there is no ligand attached to carbon, the $(Fe-C)_z$ bond is shorter than the $(Fe-C)_{xy}$ bond, and carbon is approximately collinear with the axial iron atoms; these are clearly signs of π bonding. On the other hand, products of attack of a ligand on a carbide carbon atom have no need for this stabilizing π bond. In these products, structures **12** or **13**, the average $(Fe-C)_z$ bond length equals the average $(Fe-C)_{xy}$ bond length, and carbon is not collinear with the axial iron atoms ($\theta < 180°$). Deviation from collinearity increases with increasing steric bulk of the ligand.

It is also interesting to examine what happens to our IOO curves when carbon is no longer collinear with the axial iron atoms. The IOO curve for structure **15** in Figure 3 shows us what happens when θ is 150°. The HOMO moves up in energy and has a much bigger overlap with the probe ligand. Weakening the iron-to-carbon π bond also causes the antibonding orbital to come down in energy; we see an increasing overlap of the probe ligand with low-lying acceptor orbitals such as **56**. Our numerical criterion also shows that the reactivity goes up when we decrease the angle θ at the carbon atom.

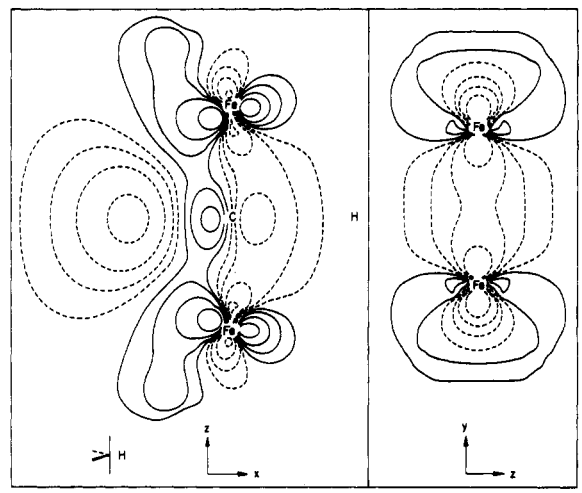

Figure 7. Contour plots corresponding to two views of the HOMO.

π bonding can also be invoked to explain the greater reactivity of a butterfly carbide carbon atom when compared to a square-pyramidal carbide carbon atom. The reason is that carbon in the latter case π bonds with four in-plane Fe atoms **20**, rather than two in-plane Fe atoms in the butterfly carbide **19**. Hence the carbon p_x orbital is more strongly stabilized, and this result is reflected in the IOO curves.

At this point a word of caution is in order. The reactivity we have referred to above is explicitly related to attack by a nucleophile. In particular, if we discuss the acidity of the carbide carbon atom in these clusters we must consider the electrophile H^+, which moves freely on and off the carbon atom. In other words acidity is often a thermodynamic phenomenon. However, our IOO curves are still useful. This is because our probe also measures the thermodynamic stability of different sites on the reactant, as is obvious from the above discussion. The point is that the conjugate anion of this acid is stabilized by π bonding, and this stabilization is greater for the Fe_5 cluster.

At this point we have shown why the carbide carbon atom is not reactive, but we have not shown why attack takes place at other sites on the cluster. To understand this it is helpful to examine some orbital plots. Clearly the nature of the HOMO is very important: it might even be able to predict the direction of nucleophilic attack. Figure 7 shows that this is so. The HOMO is shown in two views. The view in the xz plane passes through carbon, two axial iron atoms, and the center of the equatorial iron-to-iron bond. The position of the attacking probe in **12** is indicated by a H atom. This figure shows that the electron density is greater at $-x$, toward the back iron-to-iron bond, than it is at $+x$, in the direction of the attacking H atom. The other view of this orbital is a cut

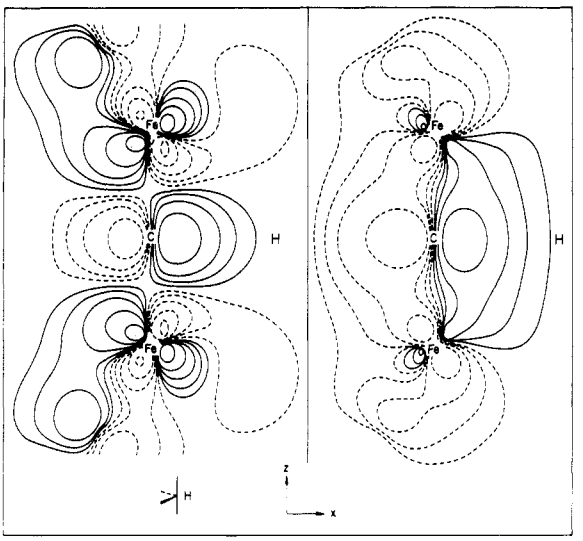

Figure 8. Contour plots of the a_1 orbitals 54 and 74.

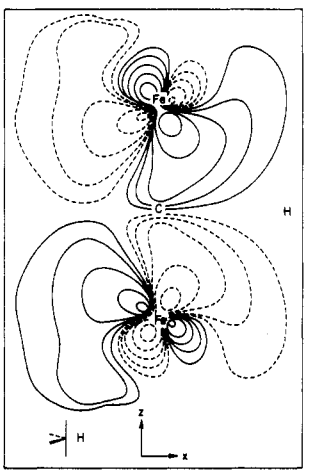

Figure 9. Contour plot of the b_2 orbital 59.

through the equatorial iron-to-iron bond (yz plane), showing that this orbital is in fact strongly bonding between these iron atoms. Hence, we correctly predict the direction of preferred attack to be on this bond.

Figure 8 shows two other a_1 orbitals, a low-lying unoccupied orbital (54) and one of the iron-to-carbon bonds (74). These were chosen because they have a relatively high component on the carbon atom. Compared to the HOMO, orbital 74 has a greater electron density at $+x$, in the direction of the attacking nucleophile, and a smaller electron density at $-x$. Hence, it is this orbital, shown schematically in **19**, that interacts preferentially with a nucleophile, in agreement with everything we have said previously. The low-lying unoccupied orbital has too many nodes to interact well with the probe, and this explains our earlier observation that a probe does not interact well with unoccupied orbitals.

If we look at the orbital just below the HOMO, Figure 9, we can explain why **13** is the second most likely mode of attack. This orbital, schematized in **21**, is essentially

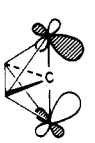

21

the minus combination of the Fe orbitals that stabilized the carbon p_x orbital in **19**. This minus combination has

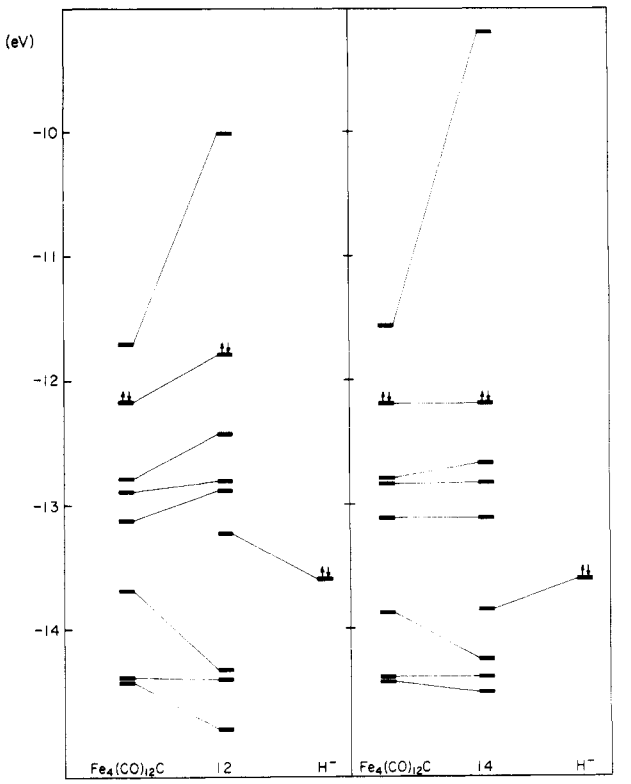

Figure 10. Interaction diagrams showing the formation of a C–H bond to the carbide carbon atom (left) and of Fe–H bonds bridging the equatorial Fe–Fe bond (right). Only orbitals of a_1 symmetry are shown.

b_2 symmetry, but it cannot interact with the carbon z orbital since it has a node approximately along the Fe–C–Fe axial thread. Hence, it is high in energy when compared to the plus combination of the same iron orbitals. In order to take advantage of this orbital, the probe has to move in the z direction and bridge an iron-to-carbon bond. This is exactly the geometry described by **13**.

VI. Electron Counting in the Product

The skeletal electron pair counting rule[18] is a marvelous device for rationalizing the structures of clusters. In applying this formalism one occasionally runs across interesting ambiguities. One example is how to count the carbide carbon atom. Experimental evidence suggests that we maintain the same electron count in the carbidic cluster as we do in the noncarbidic cluster if we count carbon as neutral, a four-electron donor. This implies that no new occupied states are introduced on interacting carbon with the rest of the cluster. The calculations of both Lauher[17] and ourselves support this statement, and we[4] considered in detail the reasons why this was so for octahedral $Ru_6(CO)_{18}C^{2+}$.

In this section we shall consider the products of attack on the carbide. In Figure 10 we have constructed interaction diagrams for attack on the carbidic carbon atom as well as on the back Fe–Fe bond. These diagrams are similar to those of Figure 4, except that the C–H (1.09 Å) and Fe–H (1.70 Å) distances have been shortened to form bonds. For attack on the back iron-to-iron bond, we also had to bend back the equatorial $Fe(CO)_3$ fragments: $\phi_2 = \phi_3 = 151.63°$.

In Figure 10, as in Figure 4, H^- interacts mainly with occupied orbitals. The result is that the HOMO is pushed up above the HOMO–LUMO gap and becomes empty. In other words the product has the same number of occupied orbitals as the reactant. We can think of this product either as attachment of a Lewis acid to $Fe_4(CO)_{12}C^{2-}$ or as

attachment of a Lewis base to $Fe_4(CO)_{12}C$.

In Table I we took the latter point of view. Here we have listed the known derivatives of $Fe_4(CO)_{12}C$ and $HFe_4(CO)_{12}C^+$ (protonated on the back iron-to-iron bond). The results justify our electron counting scheme.

We can also consider the product $HFe_4(CO)_{12}CH$ as a CH group bridged across the wings of the Fe_4 butterfly. In this case CH is a five-electron donor, because there is interaction between the C–H bond and an iron framework orbital, analogous to **19**. The point is emphasized by looking at the apparently isoelectronic compound **22**.[9]

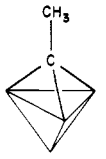

22

Since the skeleton electron count for a tetrahedral cluster is two less than that for a butterfly cluster, the out-of-plane CCH_3 group in **22** is only a three-electron donor; i.e., there is no interaction between the C–CH_3 bond and the metal framework. A smilar analysis may applied to the claimed 64-electron butterfly clusters, made by Carty.[23]

Another detail of Table I worth mentioning is the possible role of π interaction in determining the position of a ligand attached to carbon. We compared the two bridging geometries, **11** and **13**, for CO bonded to the carbide. In both cases the distance C–CO was 1.5 Å, and the distance Fe–CO was 2.0 Å. We did not include terminal CO **12**, since it was unreasonable to assume a constant C–CO distance in this case.

In this case of a π acceptor, the contribution of π orbitals to the overlap population was 0.6669 for geometry **11** and 0.5017 for geometry **13**. Since σ interaction favors structure **13**, it is possible, though not necessary, that π acceptors are found with structure **11**. Unfortunately CO has only been isolated attached to the back iron-to-iron bond, and it is probably very reactive when attached to the carbon atom. The only "ligand" in our list with structure **11** is $FeBr_2^{2-}$. $FeBr_2^{2-}$ is d^8 ML_2, a fragment derived from square-planar ML_4. Hence, it should have four low-lying nonbonding orbitals which are filled and two frontier orbitals which are empty. The best overlap is with the frontier orbitals; hence FeB_2^{2-} is a π acceptor. For the same reason, this fragment is a poor σ donor, and this fact is consistent with the product being unstable.

π interaction of acceptors with the carbide is large and positive; i.e., interaction is mainly with occupied orbitals of the carbide. The interaction of occupied orbitals on the carbide with π donors such as OCH_3^- is repulsive; hence donors have an additional reason to favor structure **13**. We note that in our electron-counting scheme the carbene is a π donor since $HNiRu_3Cp(CO)_9C^{2+}$ is isolobal with $HFe_4(CO)_{12}C^+$, and since interaction with the carbene gives a neutral product.

In concluding this section we note a recent study of bonding and reactivity in the butterfly clusters by Harris and Bradley.[24] Their theoretical work is in general in agreement with ours, with some differences as to the composition of the $Fe_4C(CO)_{12}^{2-}$ HOMO and the reasons for the axial coordination of the organic group in $Fe_4C(CO)_{12}(CCO_2CH_3)^-$.

(23) (a) Carty, A. J.; McLaughlin, S. A.; Taylor, N. J. *Chem. Soc., Chem. Commun.* **1981**, 476–477. (b) Carty, A. J.; McLaughlin, S. A.; Wagner, J. V.; Taylor, N. J. *Organometallics* **1982**, *1*, 1013–1015.

(24) Harris, S.; Bradley, J. S., submitted for publication in *Organometallics*.

VII. Application to Surface Studies

In this section we broaden the scope of our discussion. First we consider what the appropriate geometry would have to be in order to obtain a stable carbide cluster containing three metal atoms. We then search for surfaces where the local environment of carbon is similar to that in the butterfly or square-pyramidal clusters. Finally, we consider some experimental data for these surfaces.

From our previous discussion, an essential structural feature that stabilizes the carbide is having carbon in the plane of, or collinear with, some neighboring iron atoms so that π bonding to carbon can take place. This means that a geometry in which carbon sits above the plane of a three-membered ring is not reasonable (this statement is supported by calculations of Shriver[9]). More reasonable is **23**, in which an Fe–Fe bond opens up and allows carbon to bridge it. In fact, an analogous nitride does exist.[25]

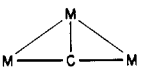

23

Similarly, we would expect that surface carbides are stabilized when carbon lies approximately in the plane of the surface layer of metal atoms. Consider the fourfold site on the (100) face of bcc, a site whose local environment resembles that of a square-pyramidal cluster. For a cube of side a, M–M = $3^{1/2}a/2$. If carbon lies in the surface layer, M–C = $a/2$, and the ratio (M–M)/(M–C) = $3^{1/2}$. For an Fe–Fe distance of 2.5 Å, Fe–C would be 1.44 Å. This means that carbon must lie ~0.5 Å outside the surface plane.

Carbon can get much closer to the surface of an fcc metal. In this case, M–M = $a/(2^{1/2})$. If Fe–Fe = 2.5 Å, Fe–C = 1.77 Å, so carbon can be 0.1–0.2 Å outside the surface layer. Further, carbon in the fourfold site on a (100) face resembles carbon in a square-pyramidal cluster, and carbon in the long bridging site on a (110) face resembles carbon in a butterfly cluster. Both of these cases are shown in **24**.

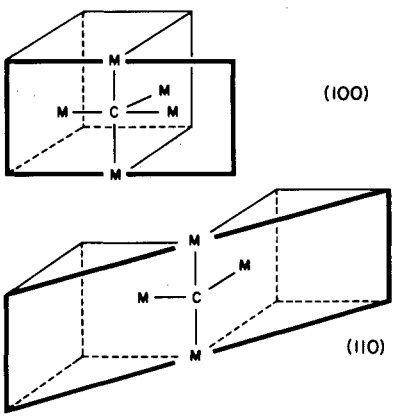

24

Unfortunately there is a paucity of good structural data for carbon attached to these surfaces. In Somorjai's[26] list of structures determined by LEED and ion-scattering techniques, we find a few examples where N or O adsorb on the fourfold sites of fcc (100). These are N on Cu, O on Co, and O on Ni. The metal-to-adsorbate distances suggest that these adsorbates are close to the surface plane of metal atoms (~0.2 Å outside this plane). It should be

(25) Feasey, N. D.; Knox, S. A. R.; Orpen, A. G. *J. Chem. Soc., Chem. Commun.* **1982**, 75–76.

(26) Somorjai, G. A. "Chemistry in Two Dimensions: Surfaces"; Cornell University Press: Ithaca, NY, 1981; pp 252–262.

noted that the analogous square-pyramidal nitride cluster[27] does exist.

Somorjai lists no examples of a small adsorbate on the long bridge site of a (110) face of a fcc crystal, although Weinberg has suggested such a site for O on Ir.[28] Nevertheless there is indirect evidence that carbon may bind to a (110) face in the manner described above. The (100) and (110) surfaces of fcc Pt, Ir, and Au are not stable; they undergo reconstruction.[29] Models for the (1 × 2) reconstruction of the (110) surface have been proposed, all of which destroy the butterfly sites for carbon.[30] What is intriguing is that small amounts of carbon have been found in many cases to stabilize the unreconstructed surface.[29,31] It is also interesting that in one of these cases carbon has been found to considerably enhance the ability of the surface to dissociate CO.[29]

Another way to have carbon on the surface is to start with a carbide. The appropriate carbides are those with the rock-salt structure exemplified by NbC. Here the metal lattice is fcc, and carbon sits in octahedral holes. Since both a square pyramid and a butterfly are fragments of an octahedron, it is clear that if the rock-salt structure is cut appropriately, carbon will have the environment we are looking for. Once again the appropriate cuts are (100) and (110), the main difference from the previous case being that the coverage of carbon is required to be 1 × 1. In the case of carbon on an fcc surface, C-C repulsion keeps the density of carbon atoms from getting as high as 1 × 1. The importance of high coverage is that in this case the butterfly or square-pyramidal "clusters" are not well isolated from one another, and this may affect their properties.

Even less is known about the surface of a carbide than about the carbonaceous surface of a metal. Rock-salt surfaces such as those of TaC and TiC have been shown to have high catalytic activity in hydrogenation as well as in Fisher-Tropsch chemistry, provided that the surfaces were activated by heating them in a vacuum.[32] In the only single crystal study on surfaces of this structure, a (111) surface in which the surface is composed entirely of metal atoms was found to be better than a (100) surface at adsorbing O_2, H_2, and N_2.[33]

Acknowledgment. We are grateful to Jane Jorgensen and Elizabeth Fields for the drawings and Sharon Drake for the typing. We also thank Timothy Hughbanks for some helpful discussion. John Bradley and Suzanne Harris kindly kept us informed of their theoretical work. Our research in this area was supported by the National Science Foundation through Research Grant DMR 7681083 to the Materials Science Center at Cornell University and by Grant CHE 7828048 and by the American Cyanamid Co.

Registry No. 1, 11087-47-1; 2, 74792-04-4.

(27) (a) Tachikawa, M.; Stein, J.; Muetterties, E. L.; Teller, R. G.; Beno, M. A.; Gebert, E.; Williams, J. M. *J. Am. Chem. Soc.* **1980**, *102*, 6648-6649. (b) Fjare, D. E.; Gladfelter, W. L. *Ibid.* **1981**, *103*, 1572-1574. (c) Fjare, D. E.; Gladfelter, W. L. *Inorg. Chem.* **1981**, *20*, 3533-3539.
(28) Weinberg, W. H.; Taylor, J. L.; Ibbotson, D. E. *Surf. Sci.* **1979**, *79*, 349-384.
(29) Nieuwenhuys, B. E.; Somorjai, G. A. *Surf. Sci.* **1978**, *72*, 8-32 and references therein.
(30) Chan, C. M.; Van Hove, M. A.; Weinberg, W. H.; Williams, E. D. *Surf. Sci.* **1980**, *91*, 440-448.
(31) (a) Somorjai, G. A. *Surf. Sci.* **1967**, *8*, 98-100. (b) Ignatiev, A.; Jones, A. V.; Rhodin, T. N. *Ibid.* **1972**, *30*, 573-591. (c) Comrie, C. M.; Lambert, R. M. *J. Chem. Soc., Faraday Trans. I* **1976**, *72*, 1659-1669. (d) Helms, C. R.; Bonzel, H. P.; Keleman, S. *J. Chem. Phys.* **1976**, *65*, 1773-1782.
(32) Kojima, I.; Miyazaki, E.; Inoue, Y.; Yasumori, I. *J. Catal.* **1982**, *73*, 128-135 and references therein.
(33) Oshima, C.; Aono, M.; Zaima, S.; Shibata, Y.; Kawai, S. *J. Less-Common Met.* **1981**, *82*, 69-74.

Transition-Metal Complexes Corresponding to the Insertion into a Group 4B Element-Carbon Bond. 3. Reactivity of Complexes with Unsaturated Carbon-Carbon Bonds. Crystal Structure of (η^5-Cyclopentadienyl)(triphenylgermyl)(η^3-hexenyl)nitrosylmolybdenum

Francis Carré, Ernesto Colomer, Robert J. P. Corriu,* and André Vioux

Laboratoire de Chimie des Organométalliques, Laboratoire Associé au CNRS No. 349, Université des Sciences et Techniques du Languedoc, 34060 Montpellier, France

Received December 28, 1983

Anions of the type $[(\eta^5\text{-}C_5H_5)(CO)(L)(M_{4B}Ph_3)M_T]^-$ (L = CO, NO; M_{4B} = Si, Ge, Sn; M_T = Mn, Mo, W) react with allyl halides, affording neutral σ-bonded alkenyl derivatives. These new complexes can rearrange to η^3-allyl complexes and also lose (allyl)M_{4B} to give η^2-allyl complexes. According to the nature of both the transition metal and the group 4B metal η^1, η^3, or η^2 complexes are obtained. A mechanism for these successive reactions is proposed. Butenyl and hexenyl iodides also react with the anions, affording η^1 complexes that can eliminate CO and rearrange to a η^3 ligand as shown by X-ray structure determination.

Introduction

In previous papers,[1,2] we reported the synthesis and reactivity of (η^5-cyclopentadienyl)transition metal anions that contain a transition metal-group 4B metal σ bond. These anions were nucleophilic enough to undergo alkylation with alkyl iodides or benzyl bromides (Scheme I). The neutral complexes thus obtained were quite unreactive (Mo, W)[1] or showed a peculiar reactivity (Mn).[2] We describe here the reactions of these anions with unsaturated halides and the reactivity of the neutral complexes thus obtained. The X-ray structure of a η^3-allylic

(1) Colomer, E.; Corriu, R. J. P.; Vioux, A. *Bull. Soc. Chim. Fr.*, in press.
(2) Colomer, E.; Corriu, R. J. P.; Vioux, A. *J. Organomet. Chem.*, in press.

0276-7333/84/2303-0970$01.50/0